MEASUREMENT OF FAULT CREEP USING MULTI-ASPECT TERRESTRIAL RADAR INTERFEROMETRY AT COYOTE DAM

Charles Werner [1], Brett Baker[2], Ryan Cassotto[3], Christophe Magnard[1], Urs Wegmüller [1], and Mark Fahnestock[4]
[1]Gamma Remote Sensing AG, Worbstrasse 225, Gümligen, 3073 Switzerland
[2]Santa Clara Valley Water District, San Jose CA, USA
[3]University, of New Hampshire, NH, USA
[4]University of Alaska, Fairbanks, AK, USA

ABSTRACT

The Calaveras fault passes directly through Coyote Dam located near Gilroy, California. The earthen structure of the dam was constructed to withstand the expected deformation due to fault creep at a rate of 10 to 15 mm/year. As part of a possible dam retrofit, the Santa Clara Valley Water District initiated a series of measurements using a Ku-Band terrestrial interferometer to accurately localize the fault trace through the dam. Measurements over the period 12-May 2016 to 18-Nov-2016 were acquired from 4 different positions situated around the down-stream face. Time series of measurements from each position were obtained after performing corrections for variable tropospheric phase delay. These measurements were combined using least-squares estimation to generate three-dimensional maps delineating both stable and rapidly deforming regions.

Index Terms— differential interferometry, terrestrial radar, tectonic deformation

1. INTRODUCTION

The Calaveras fault cuts through the southwestern side of Coyote Dam, located near Gilroy, California as shown in Figure 1. This was known in 1934 when the dam was constructed and the clay core earthen dam structure was built to withstand substantial fault motion. Now, 80 years since the dam was constructed, over 80 cm of deformation has taken place. The Santa Clara Valley Water District initiated a set of measurements of both the upstream and downstream faces of the dam using a Ku-Band terrestrial radar interferometer from February 2015 until July 2015. The dam is covered with large stable boulders making it an ideal structure for long-term deformation measurement with radar interferometry. The purpose of these radar measurements is to precisely determine the deformation zone in the dam structure. This is essential for evaluation of dam safety and planning a possible retrofit. Line-of-Sight (LOS) deformation measurements from an upstream pier were acquired approximately every 3 weeks and stacked to obtain the deformation map shown in Figure 2 [1]. The instrument is the GPRI-II real-aperture FMCW radar operating at a center frequency of 17.2 GHz with a range resolution of 0.9 meters and azimuth angular resolution of 0.38 degrees equivalent to between 1 and 2 meters in azimuth over the face of the dam [2].

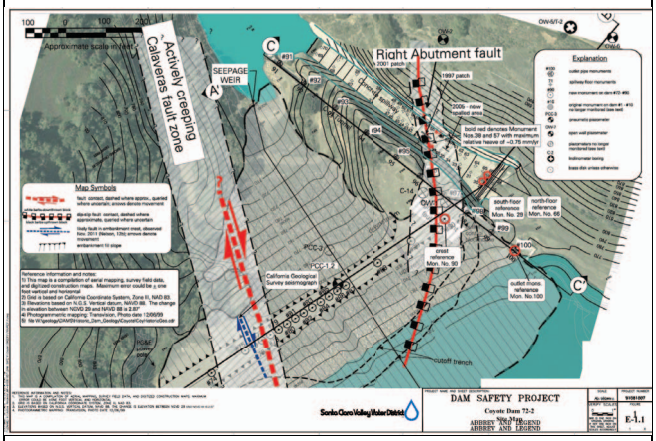

Figure 1: Fault Map of Coyote Dam showing the Calaveras Fault zone.

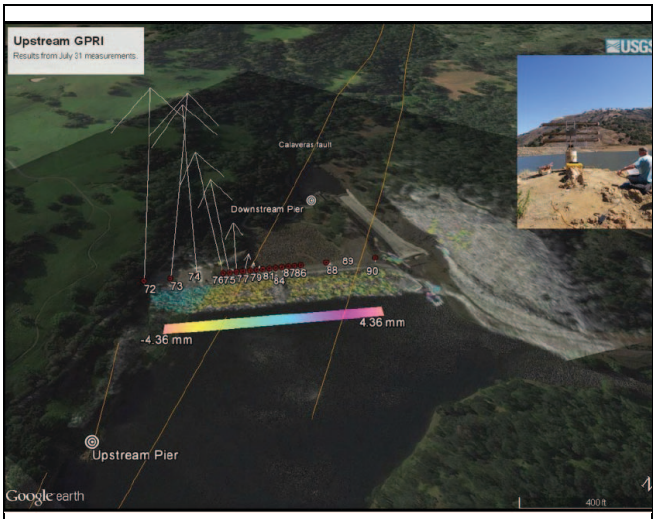

Figure 2: Upstream face deformation 20-Mar-2015 to 31-Jul-2015 showing ~3mm deformation along the line of sight.

Deformation on downstream side of the fault was measured from a single down-stream pier as shown in Figure 2. The deformation measured from the down-stream pier was inconsistent with a simple fault deformation model.

Consequently, a second campaign was proposed and approved to evaluate the deformation from multiple aspect angles to measure fault motion perpendicular to the LOS from the down-stream pier.

2. CAMPAIGN DESCRIPTION

Three additional concrete piers were set up to observe the downstream dam face. Each concrete pier stands about 1 meter above ground and permits accurate repositioning of the radar within 1-2 mm using a stainless-steel positioning plate bolted to the pier. A network of 19 corner reflectors was deployed over the dam face to facilitate accurate terrain georeferencing and coregistration of the images acquired from the different piers. The locations of the corner reflectors and pier positions are shown in Figure 3.

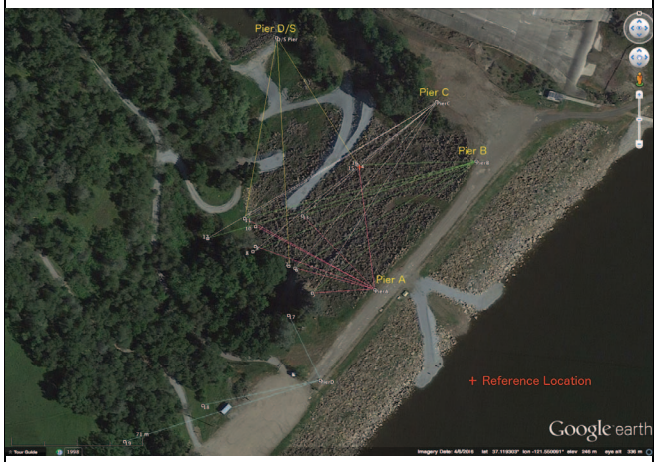

Figure 3: Pier and corner reflector positions for the extended Coyote measurement campaign. The reference point is visible from Piers A, B, C and D/S.

The new measurement positions were located along the crest of the dam looking onto the downstream face, and the original downstream position was near the dam outlet looking upstream towards the dam crest. An accurate survey was made of each pier and at each radar reflector. The corner reflectors were especially useful for confirming co-registration of the radar images. A common phase reference point was established with multiple reflectors pointing at each of the measurement piers. The reference point was selected in an area believed to be stable and clearly visible from all four piers.

The observation plan was to acquire a stack of approximately 24 images every 2 to 4 weeks at each pier. A larger number of acquisitions is preferred because it leads to reduced variations in the interferometric phase due to tropospheric water vapor and systematic phase errors due the antenna tower not being exactly vertical.

Figure 4: GPRI-II located at Pier B. Note the large rectangular silicate block close to fault plane just below the dam crest.

3. DATA PROCESSING

The GPRI-II data are acquired in polar format with distance as the radial coordinate and angle corresponding to the rotation angle of the radar. For each epoch, approximately 24 images were acquired and stacked (complex average) to improve both SNR and coherence, as well as suppress local atmospheric phase variations. The phase at the reference point was subtracted from each SLC prior to stacking, thereby effectively setting the atmosphere and deformation at the reference point to zero. Differential interferograms were then generated from the stacked SLCs, one stacked SLC per epoch.

For each date, we also stacked the detected intensity images derived from the SLCs. The averaged multi-look intensity image from the start of the observations on 12-May-2016 were terrain geocoded using a DEM obtained by LIDAR with a grid posting of 25 cm. Due to the precise survey, the only unknown is the precise value of the initial scan angle. The corner reflectors were used to determine the exact azimuth orientation.

Interferograms were produced in the series AB, BC, CD DE… where A, B, C, D… are different epochs. These interferograms were filtered and spatially unwrapped using minimum cost flow phase unwrapping algorithm.

Atmospheric related phase trends were modeled using a linear fit of the interferometric unwrapped phase in a polygonal region known to be stable. This phase model is subtracted from the interferogram phase and any residual phase offset at the reference point is also removed.

The corrected differential phases were then added together to get the time-series. A more advanced approach would be to form a network of short time interferograms and solve this

network in a least-squares sense using an SBAS based approach [4].

The times series data were then terrain geocoded and interpolated to reduce gaps between the coherent regions. Particularly at Pier A, the view angle and position was such that the downstream slope view was at a small grazing angle resulting in numerous very bright scatterers with significant shadow that made spatial phase unwrapping problematical as can be seen in Figure 5.

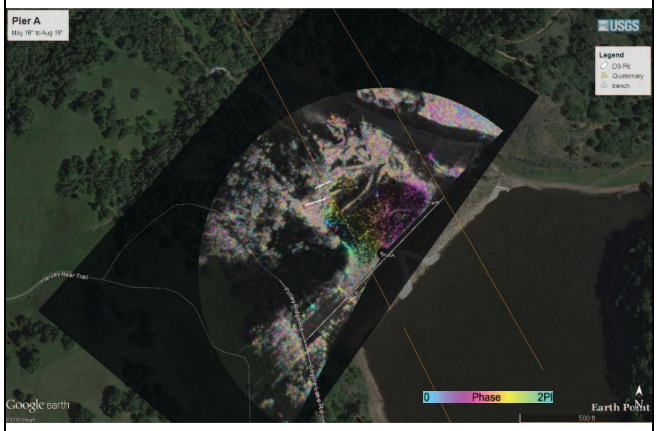

Figure 5: Terrain geocoded differential interferogram acquired from Pier A for the dates 16 May→16 August. Note the decorrelation of the phase of the vegetation.

The unwrapped phase was converted to deformation along the LOS by the simple scale factor $-4\pi/\lambda$ and then terrain geocoded. Data were acquired on the same day +/- 1 day with few exceptions. An example of the integrated deformation for 21-Oct-2016 is shown in Figure 6. The LOS deformation data are then used to solve for the three-dimensional deformation in East/North/Up (ENU) coordinates using least-squares (LS) estimation. The solution is implemented using singular value decomposition (SVD) to ensure numerical stability.

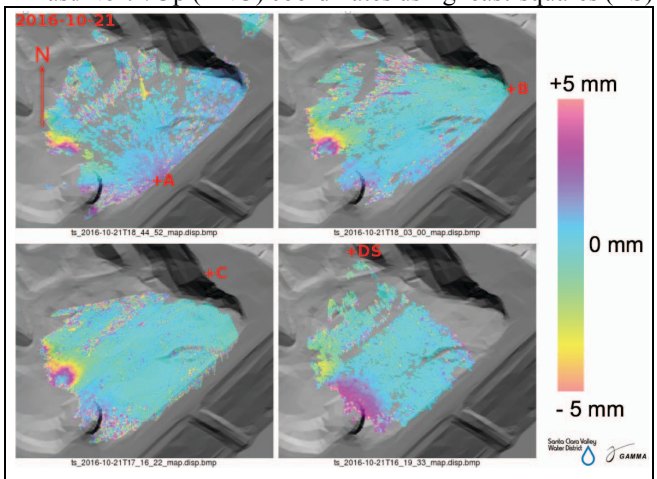

Figure 6: LOS deformation as viewed from each pier. Yellow denotes motion away from the radar.

First the look vector of each point in the scene is determined in the ENU basis. Note that the deformation measurement from a pier is the projection of the three-dimensional deformation vector onto the look vector for that position. The look vector is defined as the vector from the radar antenna phase center to the point in the scene. With 4 different positions, there are more constraints than vector components to solve for. None the less, the vertical deformation component is poorly constrained due to the near planar geometry of the 4 observation points for some parts of the scene. The projection of the LOS deformation into an orthonormal geometry can be very important for interpretation because of the rapidly changing look vector angle when close to the region of interest. This is not the case for satellite imaging. An example of a 3D deformation map is shown in Figure 7.

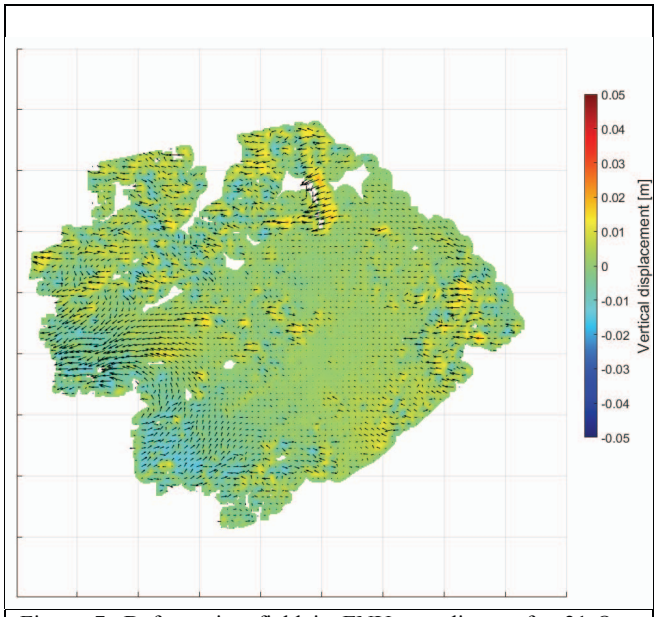

Figure 7: Deformation field in ENU coordinates for 21-Oct-2016. Color scale represents vertical deformation and the vector length is proportional to vector sum of motion in East and North directions.

4. CONCLUSIONS

It is possible to measure slow mm-scale deformation due to fault-creep or other processes using a ground-based Ku-Band band radar. The GPRI2 is particularly well suited for this application because it can be repositioned with high accuracy permitting acquisitions from multiple sites. Selection of the observation points for multi-aspect imaging is important to ensure that region of interest is clearly visible in each field of view. The stability of the boulder field covering the dam was sufficient for measurement of LOS deformation at sub-millimeter scale. The LOS deformation acquired can be

combined to solve for three-dimensional deformation time series. This study demonstrates how the data were reprojected to ENU coordinates in a frame work that can extended to include satellite, LIDAR, and GPS data. The deformation field showed significant temporal and spatial variability. The stability of large parts of Coyote Dam was confirmed. There is a region northwest of the block that is rapidly subsiding whereas the large block is both subsiding and rotating in a counter clockwise direction.

11. REFERENCES

[1] Baker, B., R. Cassotto, M. Fahnestock, C. Werner, M. Boettcher, "Measurement of Creep on the Calaveras Fault at Coyote Dam using Terrestrial Radar Interferometry (TRI)," AGU Fall Meeting 2015, https://agu.confex.com/agu/fm15/meetingapp.cgi/Paper/75970.

[2] Werner, C., A. Wiesmann, T. Strozzi, A. Kos, R. Caduff, and U. Wegmüller (2012), "The GPRI multi-mode differential interferometric radar for ground-based observations", 9th European Conference on Synthetic Aperture Radar, EUSAR, 23–26 April, Nuremberg, Germany.

[3] Caduff, R., et al. "A review of terrestrial radar interferometry for measuring surface change in the geosciences", Earth Surf. Process. Landforms 40, 208–228 (2015)

[4] Werner, C., et al. "Deformation Time-Series of the Lost-Hills Oil Field using a Multi-Baseline Interferometric SAR Inversion Algorithm with Finite-Difference Smoothing Constraints," AGU Fall Meeting 2012, San Francisco, Dec. 3-7. http://abstractsearch.agu.org/meetings/2012/FM/G43A-0910.html